ELSEVIER

Biophysical Chemistry 58 (1996) 117–124

Biophysical Chemistry

Electric birefringence of kilobase-sized DNA molecules

Nancy C. Stellwagen *

Department of Biochemistry, University of Iowa, Iowa City, IA 52242, USA

Received 19 December 1994; revised 3 May 1995; accepted 15 May 1995

Abstract

Transient electric birefringence has been used to characterize the rotational diffusion of linear, circularly permuted pBR322 and SV40 DNA molecules. The birefringence relaxation times vary with the site of linearization, suggesting that the circularly permuted DNAs have different conformations in solution. The longest relaxation times are observed for DNA sequence isomers linearized at the major bend centers identified by gel electrophoresis [1]. SV40 sequence isomers linearized at other locations have faster, but approximately equal, terminal relaxation times, suggesting that their free solution conformations are relatively independent of the location of the bend center within the sequence. By contrast, the terminal relaxation times of the various pBR322 sequence isomers vary approximately in accord with their electrophoretic mobilities in large-pore polyacrylamide gels, suggesting that the different mobilities may reflect real conformational differences between the sequence isomers.

Keywords: Electric birefringence; DNA relaxation times; DNA bending; Dynamic persistence

1. Introduction

When circular, kilobase-sized DNA molecules such as plasmid pBR322, the minichromosome SV40, or the replicative form of the bacteriophage ØX174, are linearized by single-cut restriction enzymes, sets of DNA molecules with identical molecular weights and circularly permuted sequences are produced. The circularly permuted DNAs migrate with identical electrophoretic mobilities in agarose gels, as expected for DNA molecules of identical molecular weights [1]. However, the circularly permuted DNAs migrate with different mobilities in large-pore polyacrylamide gels, suggesting that the DNAs contain sites of sequence-dependent curvature and/or anisotropic flexibility [2]. The locations of the apparent bend centers in the parent DNA molecules can be determined from the dependence of the electrophoretic mobilities of the permuted sequence isomers on the site of linearization [3]. The apparent bend angles can be estimated from the mobility differences between sequence isomers [4].

Certain small DNA restriction fragments also exhibit anomalous mobilities upon electrophoresis in polyacrylamide gels (reviewed in [1,5–7]). The mo-

* Corresponding author.

[1] N.C. Stellwagen, Electrophoresis, 15 (1995) 691.

SSDI 0301-4622(95)00091-7

bility anomalies are usually attributed to stable, sequence-dependent curvature, which is thought to impede the end-on migration of the DNA molecules through the pores of the gel [8,9]. Anisotropic, sequence-dependent flexibility may also contribute to the observed mobility anomalies [7,10,11].

Several electric birefringence and dichroism studies have been undertaken to determine whether electrophoretically anomalous DNA fragments are, in fact, stably bent or curved [12–18]. Most investigators have found that electrophoretically anomalous DNA restriction fragments exhibit faster terminal birefringence/dichroism relaxation times than electrophoretically normal fragments of the same molecular weight [19–23], suggesting that the anomalously migrating DNAs are stably bent or curved. Differences in flexibility cannot be responsible for the observed results, since the differences in persistence lengths [13,14] and/or terminal relaxation times [15,16] are independent of ionic strength. In contrast, two electric dichroism studies have found that the terminal relaxation times of electrophoretically normal and anomalous DNA fragments are indistinguishable, suggesting that the electrophoretically anomalous fragments differ only in flexibility [17,18]. It is possible that the higher electric fields used in these dichroism experiments [17,18] straightened out the inherent curvature of the electrophoretically anomalous fragments, leading to normal terminal relaxation times. Alternatively, the DNA fragments used in these particular studies may have been more flexible than the restriction fragments studied by others [12–16].

To date, no studies have been carried out to measure the apparent end-to-end lengths of linear, circularly permuted kilobase-sized DNA molecules, to see whether the variable mobilities observed in large-pore polyacrylamide gels can be attributed to intrinsically different DNA conformations. Therefore, transient electric birefringence has been used to measure the terminal relaxation times of linearized, circularly permuted sequence isomers of pBR322 and SV40 DNAs in dilute aqueous solutions. The terminal relaxation times are compared with the apparent absolute mobilities observed for the same sequence isomers in large pore polyacrylamide gels. The terminal relaxation times are also compared with other data in the literature.

2. Materials and methods

2.1. DNA samples

Plasmid pBR322 (4361 bp) and the SV40 minichromosome (5243 bp), both purchased from Gibco BRL, were linearized by digesting separate aliquots with single-cut restriction enzymes for 90 min at 37°C, using the buffer conditions recommended by the manufacturers. The completion of digestion was monitored by electrophoresis in 1.0% agarose gels. After digestion, the linearized DNAs were heated at 65°C for 15 min to inactivate the enzymes, precipitated with ethanol, redissolved in T0.1E buffer (10 mM Tris–HCl buffer, pH 8.1, plus 0.1 mM EDTA), and stored at −20°C. The electrophoretic studies are described in detail elsewhere [2,19]. For the electric birefringence measurements, aliquots of the linearized DNA stock solutions were diluted to ca. 10 μg/ml with 0.1 × T0.1E buffer, placed in the birefringence cell and equilibrated at constant temperature (20°C) for 1 h before the measurements were started.

2.2. Apparatus and methods

The electric birefringence apparatus has been described in detail previously [15]. The Kerr cell was a shortened quartz spectrophotometer cell with negligible strain birefringence. The electrodes were parallel platinum plates with a 2.0 mm separation, mounted on a lexan support of standard design [20]. Square wave pulses were generated by a Cober Electronics Model 605P high power pulser, used in the single shot mode. The pulses usually ranged from 3–7 kV/cm in amplitude and 100–400 μs in duration, just long enough to reach steady state orientation at each electric field strength. Increasing the electric field strength above 7 kV/cm, or increasing the pulse length beyond that required to reach steady state orientation decreases the relative contribution of the slowest rotational relaxation mode to the birefringence decay curves [21]. Failure to reach steady state orientation also decreases the relative contribution of the slowest decay mode [22]. To increase the signal/noise ratio under these relatively stringent operating conditions, 4–8 pulses were aver-

aged at each electric field strength, reversing the polarity between successive pulses. Typical oscilloscope traces have been selected to illustrate the results.

2.3. Data analysis

The equation describing the optical system of the birefringence apparatus is:

$$\frac{\Delta I}{I_\alpha} = \frac{\Delta V}{V_\alpha} = \frac{\sin^2(\alpha + \delta/2) - \sin^2\alpha}{\sin^2\alpha + K_{SL}} \quad (1)$$

where ΔI is the change in light intensity induced by the electric field, I_α is the light intensity observed with the analyzer rotated α degrees from the crossed position, ΔV and V_α are the corresponding output voltages from the opto-amplifier, δ is the phase retardation of the sample and K_{SL} is the stray light constant [15,28]. The analyzer was typically set at $-3°$ or $-4°$, so that the negative birefringence of DNA would produce an increase in light intensity.

The birefringence decay curves were analyzed using a non-linear least squares fitting program, CURVEFIT, based on the Marquardt algorithm [24]. The terminal relaxation times, characteristic of the overall rotational diffusion of the ensemble of DNA molecules, were independent of applied voltage over a two-fold range of electric field strength, E, if $E \leq 7$ kV/cm, and independent of pulse duration over a 50% variation in pulse length. Hence, the terminal relaxation times measured under various experimental conditions were averaged to give the values reported below; the standard deviation of the averaged values was typically ± 10–15%. The initial decay of the birefringence, presumably due to DNA bending and/or segmental motions [25–28], was not characterized quantitatively, and is not discussed here.

If the DNA molecules are assumed to be rigid and rod-like, the terminal relaxation times can be related to macromolecular length using the Tirado-Garcia de la Torre equation [29], as simplified by Elias and Eden [30],

$$\tau_{long} = \frac{\pi\eta L^3}{18kT(\ln p - 0.662 - 0.92/p)}$$

where τ_{long} is the terminal relaxation time, characteristic of the ensemble of macromolecules, L is the apparent hydrodynamic length, p is the axial ratio, and η is the viscosity of the solution. Equivalent results are obtained using the Broersma equation [31], because of the high axial ratio of the DNA molecules.

The root-mean-square average end-to-end length, L, of a wormlike-coil DNA molecule can be calculated [32,33] from its contour length, L_c, if the persistence length, P, is known or can be estimated, using Eq. (3):

$$L = \langle h^2 \rangle^{1/2} = \{2PL_c(1 - P/L_c) + P/L_c[\exp(-L_c/P)]\}^{1/2} \quad (3)$$

where $L_c = 0.34$ nm $\times$ bp. Conversely, values of L estimated from Eq. (3) can be used with Eq. (2) to calculate the terminal relaxation times expected for DNA molecules of arbitrary molecular weights.

3. Results

Typical electric birefringence signals observed for AvaI-linearized pBR322 and AccI-linearized SV40 are illustrated in Fig. 1a and b, respectively. The

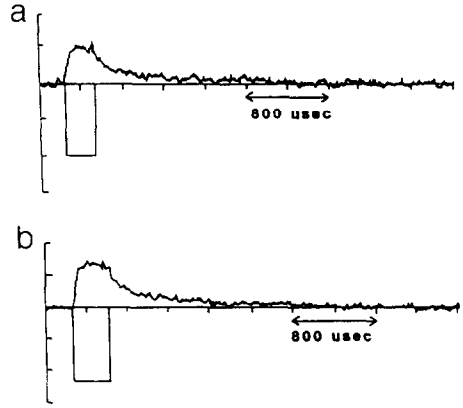

Fig. 1. Electric birefringence signals observed for (a) EcoRI linearized by AvaI, $E = 3.7$ kV/cm, pulse duration, $t_p = 310$ μs; and (b) SV40 linearized by AccI, $E = 4.8$ kV/cm, $t_p = 380$ μs. The vertical scale is arbitrary but the same for both traces; the horizontal scale is indicated. The direction of negative birefringence is up.

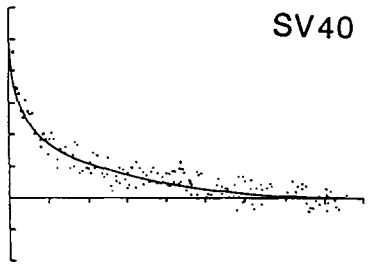

Fig. 2. Analysis of the decay of the birefringence of the SV40 trace illustrated in Fig. 1(b), using the program CURVEFIT. The solid line is the calculated fit, with terminal relaxation time, τ_{long} = 1040 μs. This component comprises 50% of the decay curve.

decay of the birefringence of the SV40 isomer is shown on an expanded scale in Fig. 2, along with the fitted curve. It can be seen that the terminal portion of the decay is reasonably well described by the fitted curve. The slowest component in the decay curve, which contributes ca. 50% of the birefringence signal, has a relaxation time of 1040 μs. Under the pulsing conditions used here, the slow component always comprised 30–50% of the birefringence signals.

The average terminal relaxation times obtained for the various sequence isomers are summarized in Table 1. The average standard deviations were typically $\pm$10–15%. If the DNA axial ratio is assumed to be ca. 100, which seems reasonable for kilobase-sized DNA molecules in dilute Tris buffers, apparent hydrodynamic lengths can be estimated for each of the sequence isomers from Eq. (2). These apparent lengths, which are given in column 5 of Table 1, range from 340–490 nm for the pBR322 sequence isomers and 440–580 nm for the SV40 sequence isomers, depending on the site of linearization. Completely stretched pBR322 and SV40 DNA molecules would have contour lengths of 1480 and 1780 nm, respectively. The corresponding relaxation times calculated from Eq. (2) would be 25 and 42 ms, respectively, more than an order of magnitude larger than the relaxation times actually observed. Hence, all the pBR322 and SV40 sequence isomers are highly coiled in solution; the different terminal relaxation times observed for the different sequence isomers reflect relatively small changes in overall DNA conformation.

Table 1
Average terminal relaxation times observed for DNAs linearized at different sites [a]

DNA	Enzyme	Site, bp	τ_{long}, μs	L, nm [b]
pBR322	EcoRI	0	1280	490
	NruI	972	430	340
	AvaI	1425	900	430
	PvuII	2066	420	340
	PvuI	3735	880	430
SV40	AccI	1628	960	440
	ApaI	2258	1020	450
	BclI	2770	2200	580
	EarI	4428	1000	450
	TaqI	4739	930	440
	BglI	5235	940	440

[a] sd = $\pm$10–15%.
[b] Calculated assuming p = 100.

The most highly stretched DNA sequence isomers, pBR322 cut by EcoRI and SV40 cut by BclI, were linearized at the sites of maximum curvature identified by the circular permutation assay [2], thus verifying the location of the major bend centers in the parent DNA molecules. Assuming that these EcoRI and SV40 sequence isomers have typical random coil conformations in solution, their terminal birefringence relaxation times can be compared with other values in the literature, as shown in Fig. 3. The relaxation times of the low molecular weight DNAs in this figure are taken from several independent electric birefringence and dichroism studies of DNA restriction fragments [21,22,34,35]. The high molecular weight data are taken from older studies in the literature, using electric birefringence [36], flow dichroism [37], or frequency-dependent electric birefringence [38] to characterize various high molecular weight DNAs. These studies were selected because the molecular weights of the DNAs were known from independent measurements.

The solid line in Fig. 3, calculated from Eq. (2) assuming L to be the DNA contour length, describes the relaxation times of restriction fragments $\leq$ 130 bp in size, which are essentially rod-like under the conditions typically used for electro-optic studies. The relaxation times of the larger DNA molecules are better described by the dashed line, which was calculated from Eq. (3) assuming an apparent persistence length of 120 nm. This apparent persistence

length is significantly larger than the persistence length of 50–60 nm calculated for small DNA restriction fragments [26,39–41]. Hence, the apparent persistence length estimated from the best fit of Eq. (3) to the electro-optic data may reflect the dynamic bending rigidity of DNA [42]. Dynamic persistence lengths ranging from 100–250 nm have been estimated by others, using a variety of methods [43–46].

The terminal relaxation times observed for the various sequence isomers of pBR322 and SV40 are compared with their electrophoretic mobilities in large-pore polyacrylamide gels in Fig. 4. For both SV40 and pBR322, the largest terminal relaxation

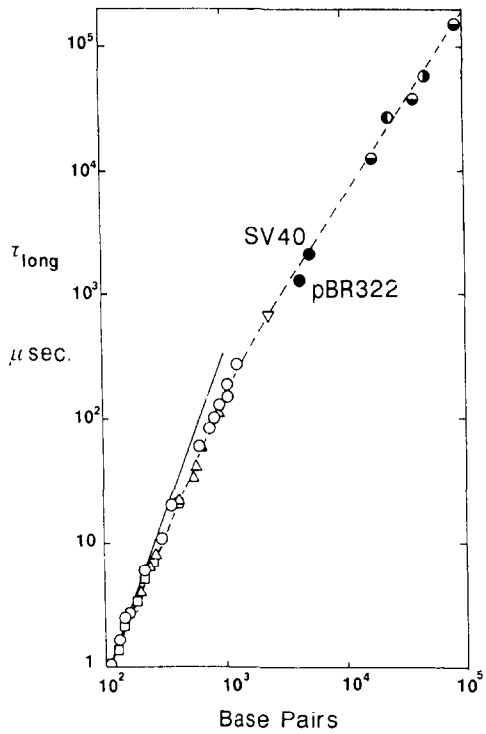

Fig. 3. Log–log plot of the dependence of the terminal rotational relaxation time, τ_{long}, on the number of base pairs in the sample. Relaxation times determined by electric birefringence or electric dichroism of DNA restriction fragments: (○), Ref. [21]; (△), Ref. [34]; (□), Ref. [35]; (▽), Ref. [22]; (●), pBR322 and SV40, present study, most extended random coil-like conformation of each DNA; (◐), electric birefringence of T7 DNA, Ref. [36]; (◒), flow dichroism of sheared T4 DNA, Ref. [37]; (◑), frequency dependent electric birefringence of salmon sperm DNA, Ref. [38]. The solid line is a plot of Eq. (2); the dashed line is a plot of Eq. (3), assuming a persistence length of 120 nm.

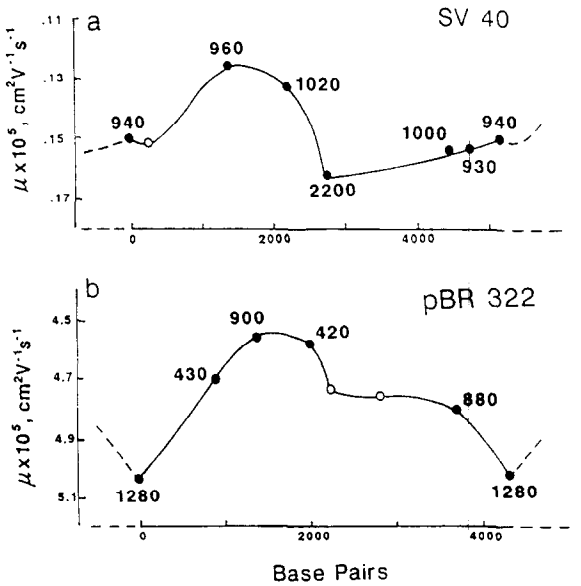

Fig. 4. Comparison of the average terminal birefringence relaxation times with the apparent absolute electrophoretic mobilities observed for sequence isomers of (a), pBR322 and (b), SV40, in a 6.9% *T*, 1% *C* polyacrylamide gel. The terminal relaxation times, in μs, are given above the site at which the DNA was linearized. The standard deviation of each of the average relaxation times is ±10-15%. The mobilities of the various sequence isomers (○) are plotted vs. the site of linearization; the solid line is drawn to guide the eye. Note that the mobilities are plotted with mobility increasing toward the bottom of the ordinate, so that the plot mimics the appearance of an electrophoresis gel. The dotted lines represent an extension of the abscissa in each direction.

times are observed for sequence isomers linearized at the major bend centers identified by the circular permutation assay (bp = 2770 and 0, respectively) [2,19], thus verifying the location of the major bend centers. The terminal relaxation times of the other SV40 sequence isomers are approximately equal (Fig. 4a), suggesting that their over-all end-to-end lengths are independent of the location of the bend center with respect to the end of the molecule.

The terminal relaxation times of the pBR322 sequence isomers vary approximately in accord with their electrophoretic mobilities (Fig. 4b). The major exception is the sequence isomer linearized at the AvaI site (bp = 1425), which exhibits a relatively long relaxation time even though it has a relatively slow electrophoretic mobility. However, this sequence isomer contains 4 unpaired bases at each end,

three of which are GC residues. Base pairing of the 'sticky ends' may have led to the formation of a small number of dimers and/or higher oligomers in the solution, increasing the terminal relaxation time. Further studies with blunt-ended pBR322 sequence isomers will be needed to resolve this discrepancy.

4. Discussion

The results in Table 1 indicate that the terminal relaxation times of linearized, circularly permuted pBR322 and SV40 DNA molecules depend on the site of linearization, suggesting that the permuted sequence isomers have different end-to-end lengths in solution. The terminal relaxation times observed for pBR322 and SV40 in their most extended, random coil-like conformations are consistent with other data in the literature, as shown in Fig. 3. The terminal relaxation times of DNA molecules with a wide range of molecular weights can be related to their contour lengths if the persistence length is taken to be 120 nm. Since this persistence length is about twice as large as the persistence length calculated for small DNA molecules [18,39–41], it may be a measure of the dynamic bending rigidity of DNA [42]. Similar values of the dynamic persistence length have been determined by others [43–46].

The pBR322 and SV40 sequence isomers that exhibit the slowest terminal relaxation times also have the fastest electrophoretic mobilities, as shown in Table 1 and Fig. 4, suggesting that linearization at these sites destroyed the major bending locus in each DNA molecule. The birefringence and electrophoresis results therefore agree in the identification of the major bend centers. These bend centers, which have also been visualized by electron microscopy [46,47], are located near the transcription terminus in SV40 [46] and at a site of divergent transcription initiation in pBR322 [48].

The terminal relaxation times of the other sequence isomers depend on the source of the DNA. SV40 sequence isomers linearized at sites other than the major bend center exhibit terminal relaxation times that are approximately independent of the site of linearization, suggesting that these sequence isomers have approximately the same end-to-end lengths in solution. The results further suggest that, except for the sequence isomer linearized at the major bend center, the different electrophoretic mobilities observed for circularly permuted SV40 sequence isomers in large-pore polyacrylamide gels cannot be attributed to intrinsic differences in DNA conformation. It is possible that sequence-dependent differences in anisotropic flexibility [10,11,49] and/or variable interactions of the SV40 sequence isomers with the polyacrylamide matrix during electrophoresis [50] may contribute to the observed differences in electrophoretic mobility. Further studies will be needed to resolve this question.

In contrast to the results observed with SV40, the terminal relaxation times observed for the various pBR322 sequence isomers approximately mirror their electrophoretic mobilities in large-pore polyacrylamide gels (Fig. 4b). Hence, the variable electrophoretic mobilities may reflect real conformational differences between the pBR322 sequence isomers. The correlation between the electrophoretic and birefringence results is not perfect, possibly because the various sequence isomers contained different numbers of unpaired bases at each end. Further studies with blunt-ended sequence isomers will be needed to resolve the ambiguities.

Apparent bend angles corresponding to the major bend centers in pBR322 and SV40 DNA may be estimated from the maximum and minimum mobilities, μ_{max} and μ_{min}, observed for the various sequence isomers, using an equation given by Thompson and Landy [4]:

$$\mu_{min}/\mu_{max} = \cos \alpha/2 \quad (4)$$

where α is the apparent deviation from the horizontal. Apparent bend angles can also be estimated from

Table 2
Estimation of apparent DNA bend angles

DNA	Bend center	Apparent bend angle	
		Electrophoresis [a]	Birefringence [b]
pBR322	0	52°	92°
SV40	2770	72°	81°

[a] Estimated from Eq. (4), averaging the mobilities observed in polyacrylamide gels containing 8.1% *T*, 0.5% *C* and 6.9% *T*, 1% *C* [2].
[b] Estimated from Eq. (5).

the minimum (L_{min}) and maximum (L_{max}) hydrodynamic lengths determined for the various sequence isomers (Table 1), if it is assumed that the major bend angle is centrally located, since:

$$L_{min} = L_{max} \cos \alpha/2 \quad (5)$$

The apparent bend angles estimated by these two methods are given in Table 2. The birefringence data (column 4) suggest that similar bend angles are found in SV40 and pBR322; the electrophoresis results suggest that the major bend angle in SV40 is considerably larger than that in pBR322. The bend angles determined by electron microscopy [46,47] are much larger than the values given in Table 2, probably because the birefringence and electrophoresis data are averages over the ensemble of conformations present in solution, while the bend angles determined by electron microscopy are selected to represent the most highly curved DNA molecules [46].

Acknowledgements

The expert technical assistance of Diana Holmes and Chia-Chen Wang in carrying out the electrophoresis experiments is gratefully acknowledged. Partial support of this work by Grant GM29690 from the National Institute of General Medical Sciences is also acknowledged.

References

[1] N.C. Stellwagen, Adv. Electrophoresis, 1 (1987) 177.
[2] N.C. Stellwagen, in R.H. Sarma and M.H. Sarma (Editors), Structural Biology: State of the Art 1993, Proceedings of the Eighth Conversations, Vol. 2, Adenine Press, Guilderland, NY, 1994, pp. 285–299.
[3] H.-M. Wu and D.M. Crothers, Nature, 308 (1984) 509.
[4] J.F. Thompson and A. Landy, Nucl. Acids Res., 16 (1988) 9687.
[5] P.J. Hagerman, Annu. Rev. Biochem., 59 (1990) 755.
[6] D.M. Crothers, T.E. Haran and J.G. Nadeau, J. Biol. Chem., 265 (1990) 7093.
[7] R.E. Harrington, Electrophoresis, 14 (1993) 732.
[8] J.C. Marini, S.D. Levene, D.M. Crothers and P.T. Englund, Proc. Natl. Acad. Sci., 79 (1982) 7664.
[9] C.R. Calladine, C.M. Collis, H.R. Drew and M.R. Mott, J. Mol. Biol., 221 (1991) 981.
[10] P.J. Hagerman, Biochim. Biophys. Acta, 1131 (1992) 125.
[11] W.K. Olson, N.L. Marky, R.L. Jernigan and V.B. Zhurkin, J. Mol. Biol., 232 (1993) 530.
[12] N.C. Stellwagen, Biophys. Chem., 15 (1982) 311.
[13] P.J. Hagerman, Proc. Natl. Acad. Sci., 83 (1984) 4632.
[14] S.D. Levene, H.-M. Wu and D.M. Crothers, Biochemistry, 25 (1986) 3988.
[15] N.C. Stellwagen, Biopolymers, 31 (1991) 1651.
[16] S.S. Chan, K.J. Breslauer, R.H. Austin and M.E. Hogan, Biochemistry, 32 (1993) 11776.
[17] S. Diekmann and D. Porschke, Biophys. Chem., 26 (1987) 207.
[18] D. Porschke, E.R. Schmidt, T. Hankeln, G. Nolte and J. Antosiewicz, Biophys. Chem., 47 (1993) 179.
[19] N.C. Stellwagen, Electrophoresis, 15 (1995) 691.
[20] R.M. Pytkowicz and C.T. O'Konski, Biochim. Biophys. Acta, 36 (1959) 466.
[21] N.C. Stellwagen, Biopolymers, 20 (1981) 399.
[22] R.J. Lewis, R. Pecora and D. Eden, Macromolecules, 19 (1986) 134.
[23] E. Fredericq and C. Houssier, Electric Dichroism and Electric Birefringence, Clarendon Press, Oxford, 1973.
[24] C.A. Swenson and N.C. Stellwagen, Biopolymers, 27 (1988) 1127.
[25] N.C. Stellwagen, in C. T. O'Konski (Editor), Molecular Electro-Optics, Marcel Dekker, New York, 1978 pp. 648–659.
[26] S. Diekmann, W. Hillen, B. Morgeneyer, R.D. Wells and D. Porschke, Biophys. Chem., 15 (1982) 263.
[27] D.B. Roitman and B.H. Zimm, J. Chem. Phys., 81 (1984) 6348.
[28] D.B. Roitman, J. Chem. Phys., 81 (1984) 6356.
[29] M.M. Tirado and J. Garcia de la Torre, J. Chem. Phys., 73 (1980) 1986.
[30] J.G. Elias and D. Eden, Macromolecules, 14 (1981) 410.
[31] S. Broersma, J. Chem. Phys., 74 (1981) 6989.
[32] H. Yamakawa, Modern Theory of Polymer Solutions, Harper & Row, New York, 1971, pp. 52–57.
[33] H. Benoit and P. Doty, J. Phys. Chem., 57 (1953) 958.
[34] P.J. Hagerman, Biopolymers, 20 (1981) 1503.
[35] J.G. Elias and D. Eden, Biopolymers, 20 (1981) 2369.
[36] D.C. Rau and V.A. Bloomfield, Biopolymers, 18 (1979) 2783.
[37] P.R. Callis and N. Davidson, Biopolymers, 8 (1969) 379.
[38] F.S. Wilkinson and G.B. Thurston, Biopolymers, 15 (1976) 1555.
[39] P.J. Hagerman, Annu. Rev. Biophys. Biophys. Chem., 17 (1988) 265.
[40] W.H. Taylor and P.J. Hagerman, J. Mol. Biol., 212 (1990) 363.
[41] C. Bustamante, J.F. Marko, E.D. Siggia and S. Smith, Science, 265 (1994) 1599.
[42] L. Song and J.M. Schurr, Biopolymers, 30 (1990) 229.
[43] S. Allison, R. Austin and M. Hogan, J. Chem. Phys., 90 (1989) 3843.
[44] J.M. Schurr, B.S. Fujimoto, P.-G. Wu and L. Song, in J.R. Lakowicz (Editor), Topics in Fluorescence Spectroscopy,

Vol. 3, Biochemical Applications, Plenum Press, New York, 1992, pp. 137–229.
[45] E.J. Hustedt, A. Spaltenstein, J.J. Kirchner, P.B. Hopkins and B.H. Robinson, Biochemistry, 32 (1993) 1774.
[46] C.-H. Hsieh and J.D. Griffith, Cell, 52 (1988) 535.
[47] G. Muzard, B. Theveny and B. Revet, EMBO J., 9 (1990) 1289.
[48] D. Stuber and H. Bujard, Proc. Natl. Acad. Sci., 78 (1981) 167.
[49] A. Bolshoy, P. McNamara, R.E. Harrington and E.N. Trifonov, Proc. Natl. Acad. Sci., 88 (1991) 2312.
[50] D.L. Holmes and N.C. Stellwagen, Electrophoresis, 12 (1991) 253 and 612.